Determination of electron temperature from spectral line intensity decay for radiation dominated plasmas

C. A. Michael[a] and J. Howard
PRL, RSPhysSE, Australian National University, Canberra A.C.T. 0200, Australia

(Presented on 21 April 2004; published 13 October 2004)

We describe a technique to absolutely estimate the electron temperature in radiation dominated plasmas from the temporal decay during the plasma afterglow of the intensity of a single spectral line. The model and underlying assumptions are described. We apply the model to data in both rf heated argon discharges and electron cyclotron heated He/H discharges in the H-1 heliac. The results agree well with probe measurements. © *2004 American Institute of Physics.*
[DOI: 10.1063/1.1787603]

I. INTERPRETATION OF SPECTRAL LINE INTENSITY

Spectral line intensities convey information about the electron density and temperature, as well as the emitting species density. Generally, collisional-radiative models are used to relate these quantities to the emission intensity. In low density plasmas, (such as those discussed here, where $n_e \sim 10^{18}$ m^{-3}), we can regard the plasma as being in coronal equilibrium. This assumption neglects the influence of metastable excitation pathways. For this model, the power radiated per unit volume into a spectral line of the primary ionic species (with upper state labeled by j and lower state labeled by i), P_{ij} can be related to the electron density n_e and electron temperature T_e through[1]

$$P_{ij} = k_{ij} n_e^2 \xi_{\mathrm{ex}}(T_e, \chi_j), \tag{1}$$

where we have set the ion density equal to n_e, valid for radiation dominated low temperature plasmas. The constant k_{ij} is dependent only on atomic rate coefficients for the particular transition, and the excitation rate coefficient $\xi_{\mathrm{ex}}(T_e, \chi_j)$ is dependent on T_e and χ_j, the excitation potential through

$$\xi_{\mathrm{ex}}(T_e, \chi_j) = T_e^{-1/2} \exp(-e\chi_j / k_B T_e). \tag{2}$$

We express the spectral line intensity as $I_{ij} = c(\lambda) P_{ij}$, where $c(\lambda)$, a wavelength-dependent calibration constant, is dependent on properties of the detector and light collection system.

The electron temperature can be obtained from spectral line ratios of the same species, based on relative calibration $c(\lambda_1)/c(\lambda_2)$.[2] For species in coronal equilibrium, this technique is sensitive to electron temperatures of the order of the difference in χ_j. However, for many species, including Ar II, the range of values of χ_j accessed by bright spectral lines is only a few eV, giving very poor sensitivity to typical values of $T_e \sim 7-20$ eV. However, line ratio methods can be used effectively for helium atoms by exploiting the significant difference in the temperature dependence of the population of singlet and triplet states.[3]

The electron temperature can also be determined given independent measurements of n_e, as well as the absolute calibration constant $c(\lambda)$. Absolute calibration can be difficult, however, since it requires an accurate knowledge of the etendue and efficiency of the optical region and absolute detector response. In practice, it is simpler to infer the absolute calibration constant $c(\lambda)k_{ij}$ from a single independent measurement of T_e (for example, from a Langmuir probe). The strong nonlinearity of $\xi_{\mathrm{ex}}(T_e)$ may result in large noise amplification.

In Sec. II, we show that when the electron power balance is dominated by radiation, the characteristic shape of the intensity decay curve depends on the electron temperature at the time the heating power is switched off and propose this as an alternative T_e measurement technique. In Sec. III, we discuss the fitting procedures and the apply this model to intensity profile data, measured using a coherence imaging camera[4,5] on the H-1 heliac.[6] The fitted temperature profiles agree well with probe measurements.

II. MODEL DESCRIPTION

The model is based on the electron power balance during the plasma afterglow, following the termination of the heating pulse. In most discharges in H−1, we find that the density decays slowly during this phase, on a time scale of the order of 3–5 ms, while the intensity decays in around 100 μs. However, in the steady state, the particle confinement time can be estimated from particle balance to be $\sim$100 μs. Since this is significantly different from the density decay time, there must be a rapid rearrangement of the plasma potential to improve particle confinement. Because the density decays much more slowly than the intensity, convective energy losses are negligible in the afterglow.

The remaining (nonconvective) electron energy loss mechanisms are radiation, ionization of neutrals and diffusive thermal transport. It is well known that in low temperature discharges, radiation can account for a substantial fraction of the total power delivered to the electrons. We consider only ionization (P_{iz}), radiation from neutrals ($P_{\mathrm{rad}}^{\mathrm{I}}$) and from ions ($P_{\mathrm{rad}}^{\mathrm{II}}$): $P_{\mathrm{tot}}(T_e) = P_{\mathrm{rad}}^{\mathrm{II}} + P_{\mathrm{rad}}^{\mathrm{I}} + P_{\mathrm{iz}}$, where each term is related to T_e, n_e, and n_n through

$$P_{\mathrm{rad}}^{\mathrm{II}}(T_e) = \sum k_{ij} n_e^2 \xi_{\mathrm{ex}}(T_e, \chi_j), \tag{3}$$

[a]Author to whom correspondence should be addressed; electronic mail: clive.michael@nifs.ac.jp

$$P^{\mathrm{I}}_{\mathrm{rad}}(T_e) = \sum k_{ij} n_e n_n \xi_{ex}(T_e, \chi_j), \tag{4}$$

$$P_{\mathrm{iz}}(T_e) = k_{\mathrm{iz}} n_e n_n \xi_{\mathrm{iz}}(T_e, \chi_{\mathrm{iz}}) \tag{5}$$

and ξ_{iz} is the ionization rate coefficient. For Ar II, the brightest spectral lines have their excitation potentials χ_j clustered around $\chi_{\mathrm{II}}=19$ eV, and for Ar I, χ_j are clustered around $\chi_{\mathrm{I}}=15$ eV.[7] Furthermore, for $T_e \lesssim 5$ eV, $\xi_{\mathrm{iz}}(T_e,\chi_{\mathrm{iz}}) \approx \mathrm{const} \times \xi_{\mathrm{ex}}(T_e,\chi_{II})$ (since $\chi_{iz}=15.75$ eV, and the classical exchange impact approximation for ξ_{iz} is close to that of ξ_{ex}[1]). This feature is not unique to argon—the excitation energies for many species are clustered around certain values. Since $\chi_{\mathrm{II}} \sim \chi_{\mathrm{I}} \sim \chi_{\mathrm{iz}}$, we take the T_e dependence of P_{tot} as being proportional (through constant b) to the excitation rate coefficient of a single ionic spectral line (which we now denote by subscript λ)

$$P_{\mathrm{tot}}(T_e) = b n_e (n_e + \alpha n_n) \xi_{\mathrm{ex}}(T_e, \chi_{\mathrm{II}}), \tag{6}$$

where $\alpha = (P^{\mathrm{I}}_{\mathrm{rad}} + P_{\mathrm{iz}})/P_{\mathrm{tot}}$.

During the afterglow, the electron stored energy decays as $dW_e/dt = P_{\mathrm{tot}}$. Expressing $W_e = n_e T_e$, and given that the density remains constant on the intensity decay time scale, we can write the following equations which can be solved self-consistently for $T_e(t)$ and $I_\lambda(t)$:

$$\frac{dT_e(t)}{dt} = b' \xi(T_e(t), \chi_{\mathrm{II}}), \tag{7}$$

$$I_\lambda(t) = c' \xi(T_e(t), \chi_{\mathrm{II}}), \tag{8}$$

$$T_e(t_0) = T_{e0}, \tag{9}$$

where $b' = b(n_e + \alpha n_n)$, $c' = c(\lambda) k_\lambda n_e^2$, and the heating power is switched off at $t = t_0$. The coefficient b' characterizes the time scale of the temperature decay, while the coefficient c' is related to the initial intensity. Consequently, discharges with higher density decay on a slower time scale and from a larger initial intensity. The relative variation of the electron density, either between discharges or across the profile, can be determined from $\sqrt{c'}$ (this effectively uses the fitted value of T_e to unfold the temperature dependence of the intensity).

The function $T_e(t)$, can be determined numerically from Eqs. (7) and (9), for a given value of b' and T_{e0}. Based on this, the intensity $I_\lambda(t)$ can be computed, given c'. Therefore, the curve $I_\lambda(t)$ can be parametrized by the three quantities T_{e0}, c' and b'. By fitting the measured decay to the model described by Eqs. (7)–(9), these three parameters can be extracted. The χ^2 residual gives an indication of validity of the approximation encapsulated by Eq. (6).

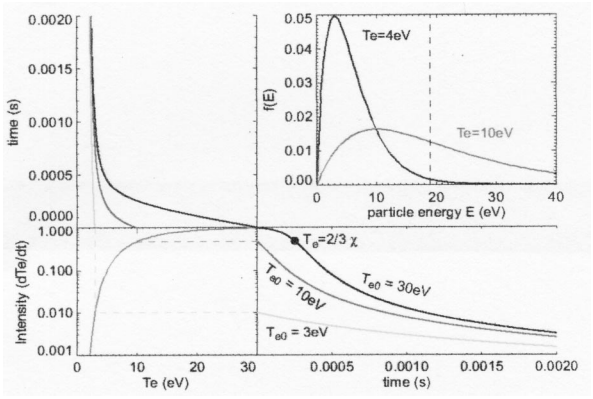

FIG. 1. Decay of electron temperature and light intensity with time, together with their coupling on the I vs T_e curve, and the distribution functions at $T_e=10$ eV and $T_e=4$ eV, showing the difference in the available populations which have energy $E>\chi$ necessary for excitation and radiative decay.

To illustrate the measurement principle, the calculated decay of the intensity and electron temperature as a function of time are shown in Fig. 1 for three initial temperatures. The characteristic shape of the light intensity decay curve depends on the initial temperature. For high T_{e0}, the rate of decrease of the intensity increases up to a point where $T_e = 2\chi/3$, then starts to decrease again, until $T_e \sim 0.1\chi \sim 2$eV, where only electrons in the tail of the distribution function have energies $E>\chi$, sufficient for radiative decay.

During the decay, the electron collision frequency is typically $\gtrsim 2\times 10^6 \mathrm{s}^{-1}$, so that for decay time scales of $\sim 50-100$ μs, at least 100 collisions can occur, thereby maintaining the distribution function Maxwellian.

III. ANALYSIS AND RESULTS

We have used the Levenberg–Macquardt method[8] for fitting the N discrete intensity measurements (t_i, I_i) to the model $I_\lambda(t)$ over the time interval $[t_0, t_0+\Delta t]$, which minimizes the weighted χ^2 residual, defined as

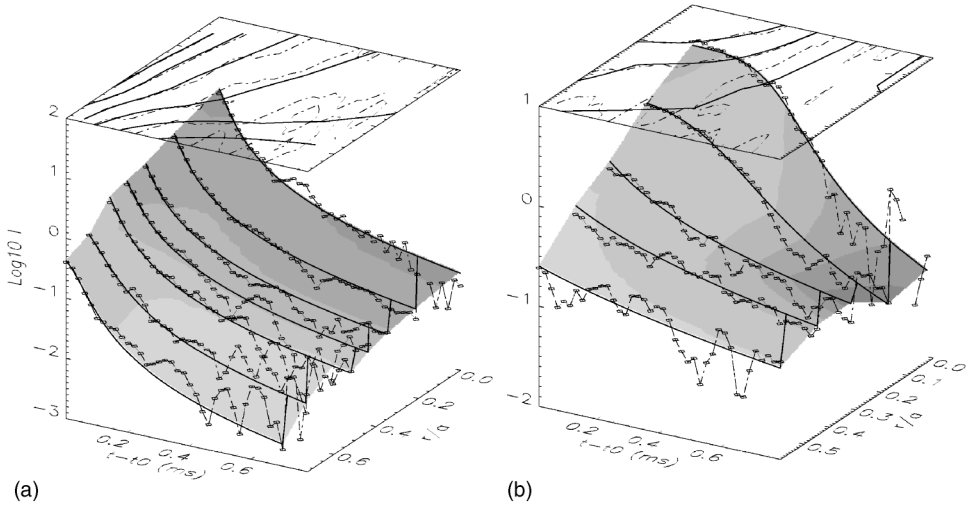

FIG. 2. Logarithm of the intensity decay for different radial positions, together with model fits, in (a) quiescent rf heated argon discharge ($B=0.09$ T, $P_{\mathrm{fill}}=36$ μ Torr, $P_{\mathrm{rf}}=60$ kW), and (b) ECRH (28 GHz, ~50 kW) He/H discharge.

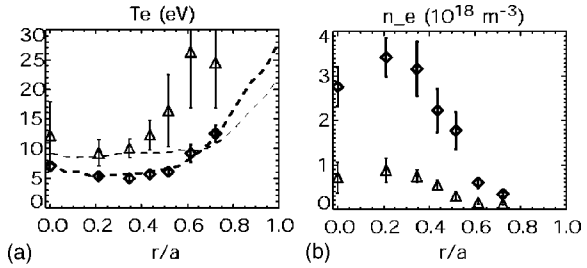

FIG. 3. Profiles of fitted electron temperature (a) and density (b), in fluctuating (triangles) and quiescent (diamonds) discharges. The fitted T_e profile is compared with probe measurements (see Ref. 9), indicated by the dashed line (thin line-quiescent; thick line-flucuating).

$$\chi^2 = \sum_{i=1}^{N} [w_i(I_i - I_\lambda(t_i)]^2. \tag{10}$$

It is necessary to make an appropriate choice for the weights w_i, the duration of the fit Δt as well as the time t_0 of the termination of the heating pulse. The Levenberg-Macquardt (LM) method[8] is used to fit the measurements $(t_i,\ I_i)$ to the model $I_\lambda(t)$ over the time interval $[t_0,\ t_0+\Delta t]$. It is necessary to make an appropriate choice for t_0 (the time of the termination of the heating pulse), the window interval Δt, as well as weighting for the fitting procedure. The time t_0 can be obtained directly by monitoring the heating power, and must be determined accurately (to within $\sim 10\ \mu$s) since the initial decay conveys most of the information about T_{e0}. For the fitting weights, we choose to minimize the absolute error. One could minimize the relative error, or incorporate the Poissonian noise directly into the weights, though in this case, the choice of Δt would affect the fitted value of T_{e0}. Furthermore, the model is less valid when the light intensity (and electron temperature) decreases to a point where radiation is no longer the dominant energy loss mechanism.

Spectral line intensities on the H-1 heliac were measured with a coherence imaging camera,[4,5] a fixed delay Fourier transform spectrometer delivering only the spectral line intensity, central wavelength and width. The instrument images a poloidal cross section of the plasma, and after signal demodulation, the data rate is 50 kHz, sufficient to track the intensity decay. We present data from three types of discharges: fluctuating and quiescent modes of rf heated argon plasmas (for which we use the Ar II line $\lambda = 488$ nm, with $\chi_{II} = 19$ eV) and an electron cyclotron resonance heated He/H discharge for which we monitor He II at $\lambda = 468$ nm (with $\chi_{II} = 54$ eV). The decay of the local (Abel inverted) intensity, together with the fitted intensity decay at various radial positions, is plotted in Fig. 2 for quiescent rf heated argon and ECRH He discharges.

Radial profiles of the fitted electron temperature and density (from $\sqrt{c'}$), in both L and H modes of rf heated argon discharges are plotted in Fig. 3. The T_e profiles are compared with probe measurements.[9] Probes are in excellent agreement with the fitted temperature profile, everywhere in the quiescent discharge, while agreeing better in the center for the fluctuating discharge. The error bars are larger in the fluctuating case due to faster decay rates (on account of lower density in spite of higher temperatures). The fluctuations themselves may also produce erroneous values of T_{e0} since this violates the model assumption of constant density. The ratio of the quiescent to the fluctuating values of the computed line integrated density $(\sqrt{c'})$ is 4.1. This compares reasonably with the value of 3.2, obtained from the 2 mm interferometer system. The agreement provides another test of the accuracy of the fitted values of T_e. The density in Fig. 3(b) was therefore absolutely calibrated based on the 2 mm interferometer. (The absolute value of the densities given are obtained from a common calibration constant, equal to the mean of the calibration constants in each case.)

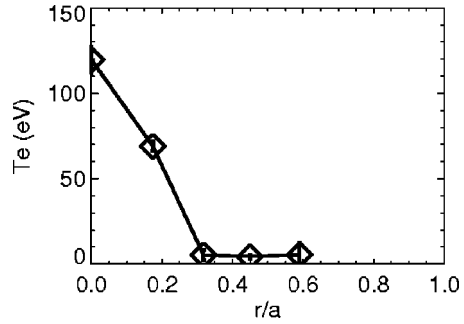

FIG. 4. Electron temperature profile for the ECRH discharge.

The fitted T_e profile for the low power ECRH discharge, plotted in Fig. 4 shows a central peaking of T_e. This feature is clearly visible in the raw data, since the central regions show light persisting much longer than for edge channels. The centrally peaked profile is characteristic of ECRH discharges, and the value of ~ 100 eV is consistent with diagmagnetic measurements, which are in the range 50–200 eV.

While the assumptions underlying the power balance in Eq. (6) are strong, this technique is useful to obtain estimates of T_e, in radiation dominated plasmas (generally where $T_e \lesssim 2\chi_{II}$). This technique has the advantage that spectral line intensities are simple to measure and no calibration procedures are required.

ACKNOWLEDGMENTS

The authors gratefully acknowledge H. Punzmann for valuable discussions, and M. G. Shats for probe data.

[1] I. H. Hutchinson, *Principles of Plasma Diagnostics* (Cambridge University Press, Cambridge, 1987).
[2] H. R. Griem, *Principles of Plasma Spectroscopy* (Cambridge University Press, Cambridge, 1997).
[3] S. Sasaki, S. Takamura, S. Watanabe, S. Masuzaki, T. Kato, and K. Kadota, Rev. Sci. Instrum. **67**, 3521 (1996).
[4] J. Howard, Rev. Sci. Instrum. **70**, 368 (1999).
[5] C. A. Michael, J. Howard, and B. D. Blackwell, Rev. Sci. Instrum. **72**, 1034 (2001).
[6] S. M. Hamberger, B. D. Blackwell, L. E. Sharp, and D. B. Shenton, Fusion Technol. **17**, 123 (1990).
[7] National Institute of Standards atomic spectroscopy database.
[8] W. H. Press, *Numerical Recipes in C: The Art of Scientific Computing* (Cambridge University Press, Cambridge, 1992).
[9] M. G. Shats, D. L. Rudakov, R. W. Boswell, and G. G. Borg, Phys. Plasmas **4**, 3629 (1997).